

1 Plaque Size Tool: an automated plaque analysis tool for simplifying and 2 standardising bacteriophage plaque morphology measurements

3
4 Ellina Trofimova¹ and Paul R Jaschke¹

5
6 Affiliations:

7 ¹ Department of Molecular Sciences, Macquarie University, Balaclava Rd, Macquarie Park NSW
8 2109, Australia

9 **Correspondence:** Paul R. Jaschke, paul.jaschke@mq.edu.au

10 **Keywords:** phage therapy, biofoundry, synthetic biology, laboratory automation, *Microviridae*,
11 Actinobacteriophages

12 **Abstract**

13 Bacteriophage plaque size measurement is essential for phage characterisation, but their
14 manual size estimation requires a considerable amount of time and effort. In order to ease the
15 work of phage researchers, we have developed an automated command-line application called
16 Plaque Size Tool (PST) that can detect plaques of different morphology on the images of Petri
17 dishes and measure plaque area and diameter. Plaque size measurements using PST showed no
18 difference to those obtained with manual plaque size measurement in Fiji, indicating future
19 results using PST are backwards compatible with prior measurements in the literature. PST can
20 be applied to a range of lytic bacteriophages producing oval-shaped plaques, including bull's-eye
21 morphology. The application can also be used for titer calculation if most of the plaques are
22 stand-alone. As laboratory automation becomes more commonplace, standardised and flexible
23 open-source analytical tools like PST will be important parts of biofoundry and cloud lab
24 bacteriophage workflows.

25 INTRODUCTION

26 Bacterial viruses, or bacteriophages, when co-plated with susceptible hosts produce clearings, or
27 plaques, of different morphology on the lawn of bacterial cells. Each plaque usually represents
28 an infection by one virus particle (1). The common plaque types include clear plaques, plaques
29 with clear centres and turbid edges (bull's-eye), plaques with a halo, and turbid plaques (2).

30 Plaques are usually visualised by co-plating phage with appropriate bacterial host strains
31 within solid media using techniques that limit phage diffusion such as using a layer of molten
32 agar or agarose matrix (overlay) (3). After incubation at a particular temperature, clearings on the
33 bacterial lawn become visible in the overlay and available for assessment and phage isolation.
34 Traditionally, plaque size was measured with a ruler or caliper (4) where the accuracy and
35 precision of the measurement depends on the skill and experience of the operator.

36 Besides being an irreplaceable part of phage isolation procedures plaque morphology is
37 essential for phage phenotypic measurements, including such fitness traits as burst size,
38 adsorption rate, and lysis time (2), and the rate of phage diffusion within a particular medium (5).
39 It is also possible to make a conclusion on the presence or absence of mutations in the phage
40 genome (6) based on changes in plaque morphology, including in rationally engineered phages
41 (7–10).

42 Currently, there are several methods for semi-automated measurement of bacteriophage
43 plaque sizes using digital images of Petri dishes. Adobe Photoshop's Ruler Tool is distributed
44 with the default software configuration and allows sizing plaque diameters in pixels but requires
45 a manual measurement. Two additional options 'Record Measurements' and 'Count tool' might
46 ease the selection of multiple objects but are only available in the extended version of Adobe
47 Photoshop, and also require manual selection (8). Alternatively, there are several free

48 applications available for viral plaque size measurement, but they all have limitations when
49 processing bacteriophage plaques.

50 One of the free phage plaque size measurement tools is Fiji (11). With ‘Oval’ and ‘Line’
51 selection tools, it is possible to manually measure the area and diameter of a plaque. The
52 ViralPlaque (12) Fiji plugin is designed to automatically detect plaques, but is only able to detect
53 plaques with clear morphology and cannot process phages that produce plaques with clear
54 centers and turbid edges (bull’s-eye morphology) like coliphage ϕ X174 and *Acinetobacter*
55 *Baumannii* phage IME200. For clear plaques, to achieve better plaque recognition by the
56 software the user is also required to adjust images manually using several settings like
57 Brightness/Contrast, Blur, and Thresholding (12).

58 Additionally, several automated and semi-automated applications were created to obtain
59 statistics on mammalian viral plaques, such as Viridot (13), Plaque 2.0 (14), Infection Counter
60 (15). However, these tools are generally used to measure the *number* of viral plaques, not their
61 *morphology*. Furthermore, some of these tools require input images obtained using specific
62 conditions (e.g. fluorescence microscopy) and are not suitable for more general uses like
63 measuring bacteriophage plaques from Petri dishes. Thus, there is currently a lack of tools
64 capable of automatically detecting and measuring bacteriophage plaques to assess their
65 morphology. To solve this issue, we created *Plaque Size Tool (PST)* that is able to detect non-
66 overlapping bacteriophage plaques on Petri dish images and measure their characteristics
67 including area and diameter, in a fully automated mode.

68 **METHODS**

69 **Bacteriophage Plaque Formation**

70 A range of wild-type and mutant ϕ X174 bacteriophage were plated using the double agar overlay
71 method as previously described (10) with *E. coli* C122 (Public Health England NCTC122)
72 grown in Phage LB (16) on 90 mm Petri dishes. The plates were incubated overnight at 37° C.

73

74 **Bacteriophage plate imaging**

75 Images of plates containing plaques of different size (one plate per one image) were taken using
76 Bio-Rad Gel Doc XR+ Gel Documentation system and Image Lab software version 6.0.1 with a
77 standard filter, white epi-illumination options and the image exposure time equal to 0.750 sec.

78 Images were exported in TIFF format in 300 (10 images) and 600 (7 images) dots per inch (DPI)
79 resolution. The dimensions of 300 DPI plates were 1606×1200 pixels, 600 DPI plates were
80 2811×2100 pixels.

81

82 **Manual plaque size measurements**

83 Plaques were manually identified and measured with Fiji version 2.1.0/1.53c using the
84 ‘Analyze/Measure/Oval’ feature. Each image was magnified up to 400% prior to the
85 measurement, and plaques were manually circled with the ‘Oval’ feature. The identifiers of
86 plaques were assigned in the same order as on the PST output image using ‘Analyze/Tools/ROI
87 Manager’. After all plaques were selected, their ‘Area’ measurements were taken using the
88 Region of Interest (ROI) Manager and exported into CSV for further analysis.

89

90

91 **Statistical analysis**

92 To compare automatically detected plaque area values using PST with manually measured
93 plaques in Fiji, plate images were divided into three groups: 300 DPI (n=10), 600 DPI (n=7), and
94 all plates (n=17). Obtained plaque size values were tested for normal data distribution with the
95 Shapiro-Wilk normality test in ‘jamovi’ (17). Plaque area values in square pixels were compared
96 between PST and Fiji in pairs where the same plaque had the same identifier in PST and Fiji.
97 The Wilcoxon signed rank test was used to compare the groups with Python 3 (18) scripting
98 using the module ‘wilcoxon’ from the package `scipy.stats` (version 1.5.4) (19). For small plaque
99 size determination, an average diameter of plaques was calculated from the plates that contained
100 noticeably smaller plaques and were measured with the ‘-small’ flag.

101 The number of correctly identified plaques by Plaque Size Tool was measured for each
102 plate to compare with the total number of non-overlapping plaques counted manually and obtain
103 the tool accuracy. All extra objects detected as plaques (false positives), along with incorrectly
104 measured plaques, were considered as not accurately identified and not included in the
105 comparison of area values. PST accuracy values for the average PST plaque diameter calculated
106 for each plate were analysed using a linear regression method (`linregress`) from the package
107 `scipy.stats` (version 1.5.4) (19).

108

109 **Plaque Size Tool development and distribution**

110 The command-line tool PST was written in Python 3 using the Open Source Computer Vision
111 Library (OpenCV) ver. 4.5.1.48 library for object detection (20). The tool is available on GitHub
112 at https://github.com/ellinium/plaque_size_tool under Apache License 2.0. The installation
113 documentation is specified in the manual (File S1) and on the GitHub webpage.

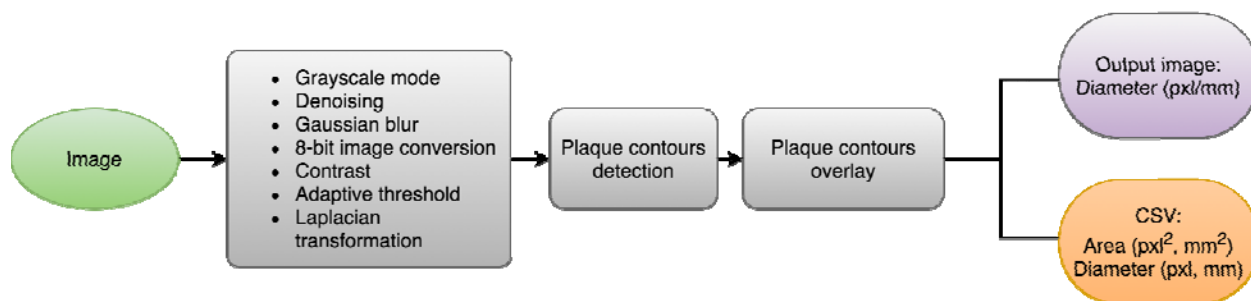
114 PST currently receives three input arguments (also called flags): (1) the full path to an
115 image (-i) or full path to a directory with images (-d) (required), (2) plate size in millimetres (-p)
116 (optional), and (3) a flag for processing small plaques (-small) (optional). The tool supports
117 images containing one Petri dish in JPG, JPEG, TIF, TIFF and PNG formats.

118

119 **Plaque Size tool image processing workflow**

120 All following methods of image transformation belong to OpenCV–Python library (21). First,
121 each image that contains only one Petri dish is converted to grayscale mode and denoised using
122 the non-local means denoising algorithm (Fig. 1). After that, the image is blurred using a
123 Gaussian blur method. The output image is then converted to an 8-bit image, and its contrast is
124 increased. In order to detect the contours of the plaques, adaptive threshold and Laplacian
125 transformation are applied. A binary image with oval contours is then formed. The image is
126 processed further to find all image contours in a two-level hierarchy structure that have all
127 external contours (i.e. its boundary) placed in hierarchy 1 and all the contours inside an object in
128 hierarchy 2.

129



130

131 **Fig. 1.** Workflow of Plaque Size Tool. The green filling colour indicates input files, grey indicates image-processing
132 steps. Purple and orange colours indicate output files. Pxl (pixel), mm (millimetre).

133

134 After all contours are found, convex hulls are drawn for a set of points of each contour.
135 Based on the hull values, a plaque area is calculated in square pixels (pxl²). A plaque diameter is
136 also calculated in pixels using the formula $2x\sqrt{\frac{Area (pxl^2)}{\pi}}$. The Petri dish contour is used to
137 convert the area and diameter of plaques from pixels to millimetres if the ‘-p’ (plate size) flag is
138 specified.

139 **Plaque Size Tool output files**

141 The detected plaque contours are drawn on the high-contrast image in green colour and saved
142 into an output folder ‘out’ that is created automatically in the directory PST is launched from.
143 Additional information is saved into a comma-separated file (CSV) and contains plaque
144 identifiers (INDEX_COL) that corresponds to the identifier of the same plaque on the output
145 image, plaque area in pixels (AREA_PXL), and plaque diameter in pixels (DIAMETER_PXL).
146 If the -p flag is used during PST execution, then plaque area in millimetres (AREA_MM), and
147 plaque diameter in millimetres (DIAMETER_MM) are also returned in the CSV file.

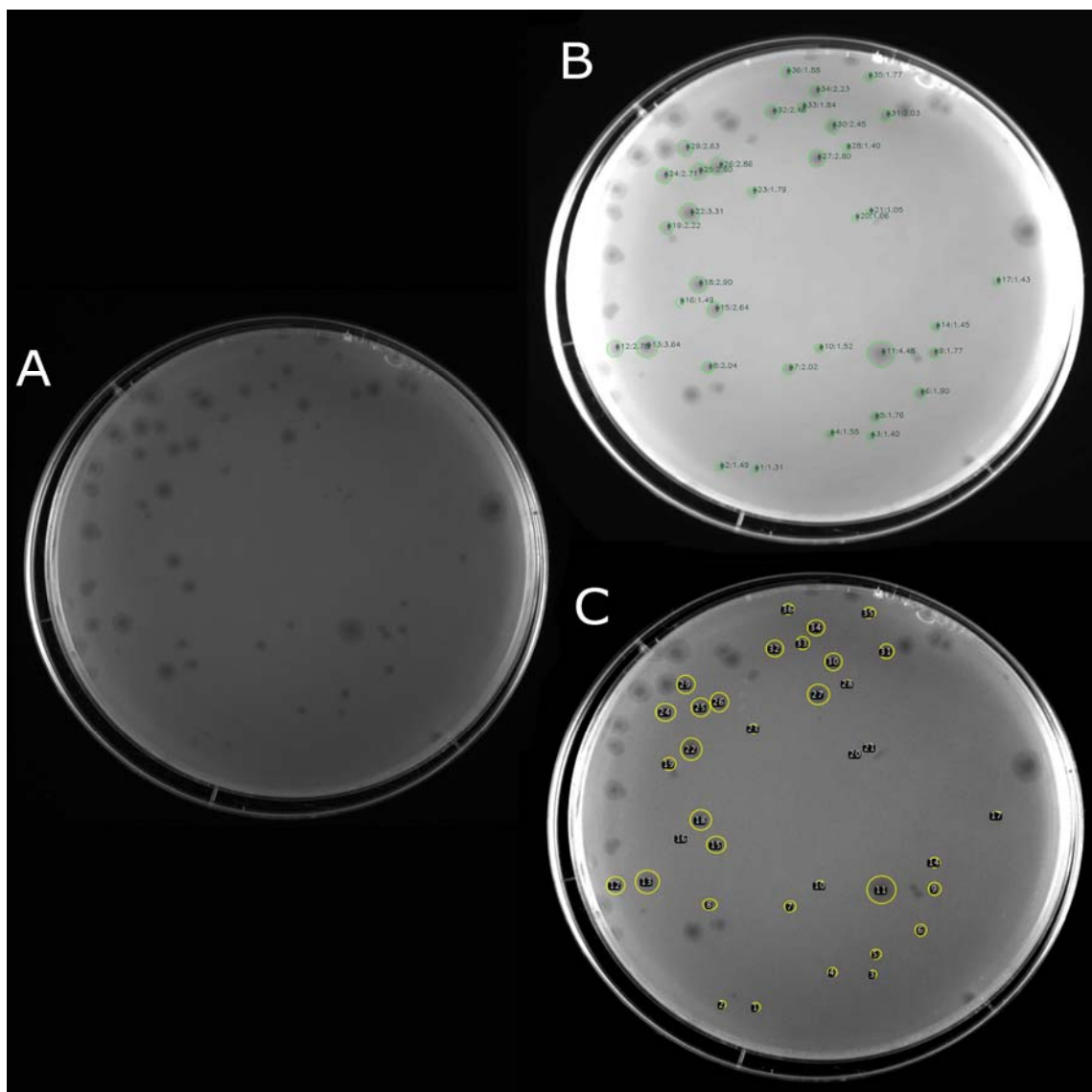
148 **RESULTS**

149 **Plaque Size Tool accuracy and detection capability**

150 Plaque Size Tool (PST) was designed to measure non-overlapping plaques from digital images
151 of double agar overlay plates. The command-line tool was developed in Python 3 using Open
152 Source Computer Vision Library (OpenCV). The tool is run with three input arguments: (1) the
153 full path to an image (-i) or full path to a directory with images (-d) (required), (2) plate size in
154 millimetres (-p) (optional), and (3) a flag for processing small plaques (-small) (optional).

155 Although PST is able to identify the contours of overlapping plaques, we chose to not use
156 these plaques for determination of plaque morphology because the size of a plaque can be
157 affected by its adjacent neighbour. The output of the tool is an image with recognized and
158 measured plaques circled and labelled with a hash (#) symbol, unique identifier separated from
159 diameter value with a full colon, and a CSV file containing area and diameter values for every
160 identified plaque (Fig. 2).

161 PST was first tested by processing 17 Petri dish images in 300 and 600 DPI resolution
162 TIFF format from experiments on phage ϕ X174 plaques in our lab (Table S1). Seven plates
163 containing visibly small plaques were processed with the '-small' flag. The images contained a
164 total of 601 non-overlapping plaques as identified by manual measurements. On average PST
165 was able to identify and measure 83.0% (499/601) of plaques across the dataset (Table S3). At
166 the plate level, detection accuracy varied between 52-100% (Table S1).



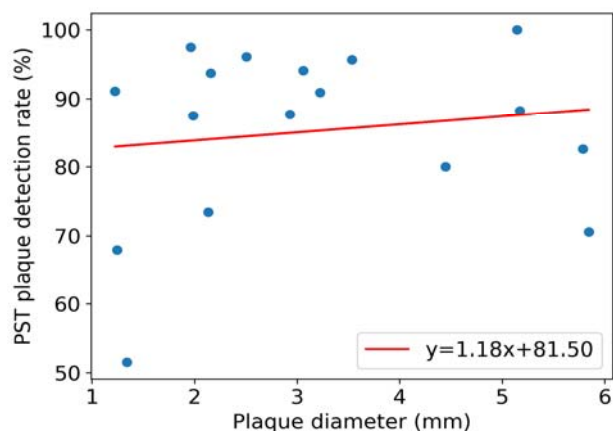
167

168 **Fig. 2.** Petri plates with bacteriophage plaques before and after analysis with plaque measurement tools. (A) The
169 original image in TIFF format. (B) An output image created by Plaque Size Tool. Detected plaques are circled with
170 green colour and labelled with a hash symbol (#) followed by a unique numeric identifier and the plaque diameter in
171 mm (e.g. #23:1.79). (C) Manual plaque selection in Fiji of the same image.

172

173 Detection accuracy did not correlate with plaque size. Mean PST plaque diameter was
174 measured for each plate and this was compared to the PST detection rate. Using linear regression
175 analysis against these data we found no correlation between the PST plaque detection rate and

176 the average plaque diameter on a Petri dish ($R^2=0.02$, slope=1.18) (Fig. 3).



177

178 **Fig. 3.** Correlation between PST plaque detection rate and the average plaque diameter. The linear least-squared fit
179 equation is provided for the method.

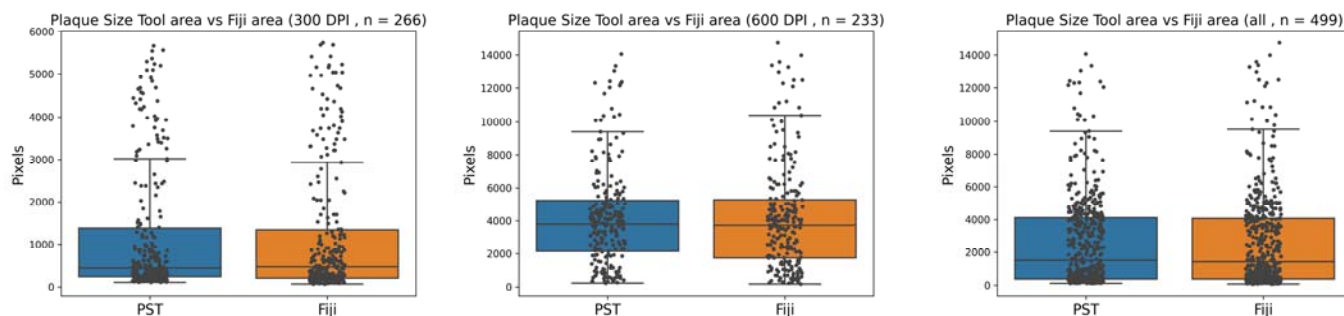
180

181 **Comparison to manual plaque measurement method**

182 We next benchmarked the PST against Fiji to determine how similar the calculated morphology
183 values between these two tools are. The values of area obtained by PST from the CSV output file
184 for each Petri dish were compared with the area values obtained by manual plaque measurement
185 on the same Petri dish with 'Analyze/Measure/Oval' feature in Fiji. Comparing the distribution
186 of measured plaque sizes between PST and Fiji showed the two methods generate very similar
187 results (Fig. 4).

188

189



190

191 **Fig. 4.** Measured plaque areas from automated PST and manual Fiji analysis shows no statistical
192 difference. (A) 300 DPI. (B) 600 DPI. (C) All. Box plots for the three plate groups with individual data
193 points overlaid. Significance of plaque area difference between conditions was measured using the
194 Wilcoxon signed rank test (18).

195

196 As the plaque area measurements are not normally distributed (Table 1) we used the

197 Wilcoxon signed rank test to compare the sizes of non-overlapping plaques measured

198 automatically by PST paired with the manually measured in Fiji. The comparison showed there

199 was no significant difference between the plaque sizes measured by PST and Fiji (Fig. 4) at the

200 0.05 significance level (Table 2).

201

202 **Table 1.** Tests for normality of PST plaque area values.

Image Group	W value	p-value
300 DPI	0.926	<0.001
600 DPI	0.962	<0.001
All	0.968	<0.001

The normality of data distribution was tested with the Shapiro-Wilk normality test in 'jamovi' (17).

Table 2. Wilcoxon signed rank test results for PST compared to manual Fiji plaque area measurements.

Image Group	W value	p-value
300 DPI	24515.500	0.674
600 DPI	13397.000	0.821
All	98774.500	0.283

The Wilcoxon signed rank test was used to compare the groups with Python 3 (18) scripting using the module 'wilcoxon' from the package `scipy.stats` (version 1.5.4) (19).

The effect of image resolution and type on plaque detection

To determine the effect of image resolution on plaque detection rate, seven plates that were previously analysed from 600 DPI resolution TIFF images group were instead exported as 300 DPI TIFF images and analysed with PST. We found on average that the number of detected plaques in the 300 DPI images was reduced from the 600 DPI images by 31 %. The reduction ranged from 4.4 % to 57.7%, depending on the plate, without correlation with the plaque size ($R^2=0.0001$, slope=0.17).

To test the ability of PST to measure plaque sizes from a range of digital images and phage we downloaded seven random plate images from the Actinobacteriophage database (22). The images were captured by a range of different cameras, including mobile phones, and had a range of different resolutions (Table S2). For the seven additional Actinobacteriophage plates, PST was able to detect 88.1% of plaques on the plates with plaques larger than 1 mm (133/151). On plates of Arthrobacter phage Rizwana plaques with sizes less than 1 mm PST detected 54.5 % (12/22) using the `-small` flag. A high proportion of plaques, 72-88%, were detected on the JPG and PNG plate images of low resolution and size (150 DPI and 413x310 pixels, 72 DPI and

624x462 pixels, and 144 DPI and 646x626 pixels) indicating that PST application can effectively process images of low resolution and size from a range of devices (Table S2).

DISCUSSION

Manual measurement of phage plaque dimensions can be tedious, time-consuming, lead to erroneous calculations, and is non-standardised. In order to ease the work of phage scientists, we created an automated command-line tool for phage plaque detection and assessment of their diameter and area parameters. Easily installed Plaque Size Tool, written in Python 3, allows single and batch image processing of bacteriophage plaques on Petri dishes in a wide range of resolutions and file formats. The tool can be applied to various lytic phages producing plaques of different morphology: clear and turbid plaques, plaques with halo, and plaques with clear centres and turbid edges (bull's-eye morphology). Only non-overlapping plaques are included in the measurement as the size of merged plaques is affected by their neighbour.

The tool can detect between 70 and 100 % of plaques on a Petri dish with plaques of diameter >1.5 mm, and 51-91 % of plaques <1.5 mm. The difficulty for plaque detection occurs on the edges of Petri dishes due to the change of an image exposure during its processing. However, even for plaques less than 1 mm, the detected plaque number on most Petri dish images is sufficient for robust calculation of size, especially considering that such plaques are very difficult to measure manually. For TIFF images, resolution lower than 600 DPI decreases plaque detection rates by PST but other image formats seem to perform better than TIFF at a range of lower resolutions which might be linked to the original contrast and brightness of the image. If an image simultaneously has a low resolution and size, the '-small' flag can be used to process such image with PST.

PST is highly accurate if compared with measurements performed manually, and the results are reproducible for each processed image as the detection algorithm will always produce the same plaque count and size measurements from the same input image.

Plaque size measurements using PST were statistically indistinguishable from those we measured with manual plaque size measurement tool Fiji (Fig. 4). As a result, PST measurements can be directly compared with past manual Fiji measurements, enabling backwards compatibility with prior literature values.

The tool can also be used for phage titer calculation with no modification if most of the plaques on the plate are not overlapping or around the edge. Alternatively, a user can manually calculate a number of plaques that were not labelled by PST (i.e., merged plaques or those around the edge) and add it to the total number of plaques calculated by the tool.

To summarise, we have created a tool that addresses a gap within the current offerings for automated phage plaque analysis. It requires minimal user actions and can process a range of Petri dish images of different format and resolution in single and batch mode. Computational tools such as PST will be an increasingly important component within analytical pipelines for phage engineering and novel phage isolation and characterisation in cloud labs and biofoundries in the future (23,24).

Author statements

Funding information

PRJ is supported by NHMRC Ideas Grant APP118539.

Acknowledgements

We thank Ilya Trofimov for elucidating features of OpenCV library and Russell M Vincent for helpful discussions. Russel M Vincent and Bradley W Wright provided the ϕ X174 bacteriophage images.

Authors and contributors

The contributions of authors of this work according to the CRediT contribution taxonomy were:

ET: conceptualization; data curation; formal analysis; investigation; methodology; software; visualization; writing-original draft; writing-review and editing.

PRJ: conceptualization; funding acquisition; project administration; supervision; writing-review and editing.

Conflicts of interest

The authors declare that there are no conflicts of interest.

References

1. Kleczkowski A, Kleczkowski J. The Ability of Single Phage Particles to Form Plaques and to Multiply in Liquid Cultures. *J Gen Microbiol*. 1951 May 1;5(2):346–56. doi: 10.1099/00221287-5-2-346
2. Abedon ST. Detection of Bacteriophages: Phage Plaques. In: *Bacteriophages*. Cham: Springer International Publishing; 2018. p. 1–32. doi: 10.1007/978-3-319-40598-8_16-1
3. Kropinski AM, Mazzocco A, Waddell TE, Lingohr E, Johnson RP. Enumeration of Bacteriophages by Double Agar Overlay Plaque Assay. In 2009. p. 69–76. doi: 10.1007/978-1-60327-164-6_7
4. Reddy MS, Reinbold GW, Hammond EG. Simplified, Rapid Method to Measure Diameter of Bacteriophage Plaques. *J Food Prot*. 1982 Feb 1;45(2):143–4. doi: 10.4315/0362-028X-45.2.143
5. Abedon ST, Yin J. Bacteriophage Plaques: Theory and Analysis. In: Clokie MRJ, Kropinski AM, editors. *Totowa, NJ: Humana Press; 2009. p. 161–74. (Methods in Molecular Biology; vol. 501)*. doi: 10.1007/978-1-60327-164-6_17
6. Spanakis E, Horne MT. Co-adaptation of *Escherichia coli* and Coliphage vir in

- Continuous Culture. *Microbiology*. 1987 Feb 1;133(2):353–60. doi: 10.1099/00221287-133-2-353
7. Jaschke PR, Lieberman EK, Rodriguez J, Sierra A, Endy D. A fully decompressed synthetic bacteriophage ϕ X174 genome assembled and archived in yeast. *Virology*. 2012;434(2):278–84. doi: 10.1016/j.virol.2012.09.020
 8. Jaschke PR, Dotson GA, Hung KS, Liu D, Endy D. Definitive demonstration by synthesis of genome annotation completeness. *Proc Natl Acad Sci*. 2019 Nov 26;116(48):24206–13. doi: 10.1073/pnas.1905990116
 9. Ando H, Lemire S, Pires DP, Lu TK. Engineering Modular Viral Scaffolds for Targeted Bacterial Population Editing. *Cell Syst*. 2015 Sep;1(3):187–96. doi: 10.1016/j.cels.2015.08.013
 10. Wright BW, Ruan J, Molloy MP, Jaschke PR. Genome Modularization Reveals Overlapped Gene Topology Is Necessary for Efficient Viral Reproduction. *ACS Synth Biol*. 2020 Nov 20;9(11):3079–90. doi: 10.1021/acssynbio.0c00323
 11. Schindelin J, Arganda-Carreras I, Frise E, Kaynig V, Longair M, Pietzsch T, et al. Fiji: an open-source platform for biological-image analysis. *Nat Methods*. 2012 Jul 28;9(7):676–82. doi: 10.1038/nmeth.2019
 12. Cacciabue M, Currá A, Gismondi MI. ViralPlaque: a Fiji macro for automated assessment of viral plaque statistics. *PeerJ*. 2019 Sep 24;7:e7729. doi: 10.7717/peerj.7729
 13. Katzelnick LC, Coello Escoto A, McElvany BD, Chávez C, Salje H, Luo W, et al. Viridot: An automated virus plaque (immunofocus) counter for the measurement of serological neutralizing responses with application to dengue virus. *PLoS Negl Trop Dis*. 2018;12(10):1–20. doi: 10.1371/journal.pntd.0006862
 14. Yakimovich A, Andriasyan V, Witte R, Wang I-H, Prasad V, Suomalainen M, et al. Plaque2.0—A High-Throughput Analysis Framework to Score Virus-Cell Transmission and Clonal Cell Expansion. Schildgen O, editor. *PLoS One*. 2015 Sep 28;10(9):e0138760. doi: 10.1371/journal.pone.0138760
 15. Culley S, Towers G, Selwood D, Henriques R, Grove J. Infection Counter: Automated Quantification of in Vitro Virus Replication by Fluorescence Microscopy. *Viruses*. 2016 Jul 21;8(7):201. doi: 10.3390/v8070201
 16. Rokyta DR, Abdo Z, Wichman HA. The genetics of adaptation for eight microvirid bacteriophages. *J Mol Evol*. 2009;69(3):229–39. doi: 10.1007/s00239-009-9267-9
 17. The jamovi project (2021). jamovi (Version 1.6) [Computer Software]. Retrieved from <https://www.jamovi.org> [Internet]. 2021.
 18. Van Rossum G, Drake FL. Python 3 Reference Manual. Scotts Valley, CA: CreateSpace; 2009.
 19. Virtanen P, Gommers R, Oliphant TE, Haberland M, Reddy T, Cournapeau D, et al. SciPy 1.0: fundamental algorithms for scientific computing in Python. *Nat Methods*. 2020 Mar 3;17(3):261–72. doi: 10.1038/s41592-019-0686-2
 20. Bradski G. The OpenCV Library. Dr Dobb's J Softw Tools. 2000;
 21. Howse J. OpenCV Computer Vision with Python. Packt Publishing; 2013.
 22. Russell DA, Hatfull GF. PhagesDB: the actinobacteriophage database. Wren J, editor. *Bioinformatics*. 2017 Mar 1;33(5):784–6. doi: 10.1093/bioinformatics/btw711
 23. Weynberg KD, Jaschke PR. Building Better Bacteriophage with Biofoundries to Combat Antibiotic-Resistant Bacteria. 2019;00(00):1–4. doi: 10.1089/phage.2019.0005
 24. Bates M, Berliner AJ, Lachoff J, Jaschke PR, Groban ES. Wet lab accelerator: A web-

based application democratizing laboratory automation for synthetic biology. ACS Synth Biol. 2017;6(1):167–71. doi: 10.1021/acssynbio.6b00108